

Analysis of front side dynamics in laser flash analysis: modeling and adjustment for enhanced thermophysical insights

Amir Narymany Shandy¹, Matthias Zipf¹, Frank Hemberger², Jochen Manara², Thomas Stark², Jürgen Hartmann^{1,2}

¹Technical University of Applied Sciences Würzburg-Schweinfurt, Münzstraße 12, Würzburg, Germany

²Center for Applied Energy Research e.V., Magdalene-Schoch-Straße 3, Würzburg, Germany

Abstract

The Laser Flash Analysis (LFA) has established itself as a reliable method for determining the thermal diffusivity of materials. In order to expand the measurement range of LFA, the investigation of the temperature development on the surface of the sample facing the laser, referred to as the front side, comes into focus. Initially, an adiabatic front-side model is applied. This model provides a fundamental approximation of the temperature distribution on the front side of the sample. To account for the high dynamics of the front-side temperature caused by the pulsed energy input of the laser, modification of the evaluation models is necessary. In this regard, the temporal evolution of the front-side temperature caused by a Dirac shaped energy input is convoluted with laser pulses of different shapes. This convolution enables a detailed investigation of the effects of various laser pulse shapes on the temperature evolution on the front side. Not only the maximum temperature is considered, but also the temporal evolution of the temperature. The choice of laser pulse shape proves to be a critical aspect, as it significantly influences the response signal of the front side. Two different convolution methods are compared using numerical solution. On one hand, convolution by multiplication in the Fourier domain using Fast Fourier Transformation followed by inverse transformation, and on the other hand, an analytical solution through the convolution integral. Both resulting curves are tested for their robustness and applicability through parameter variations.

Keywords: Laser Flash Analysis, Front side detection, additive manufacturing, multi layer samples, one layer samples

Introduction

Laser Flash Analysis (LFA) is a powerful technique for characterizing the thermo-physical properties of materials. In the context of additive manufacturing, selective laser melting (SLM) opens up new opportunities for material development and optimization of manufacturing processes. In SLM (see Fig. 1), components are built layer by layer from metal powder by selectively melting the powder with a laser to create the desired shape. The quality and properties of these additively manufactured components depend heavily on the thermo-physical properties of the materials used. Laser Flash Analysis enables the measurement of thermal conductivity and heat capacity of materials by directing short laser pulses onto the surface of the material and measuring the resulting temperature changes [1]. This data provides important insights into the heat transfer and solidification behavior of metal powders during the SLM process.

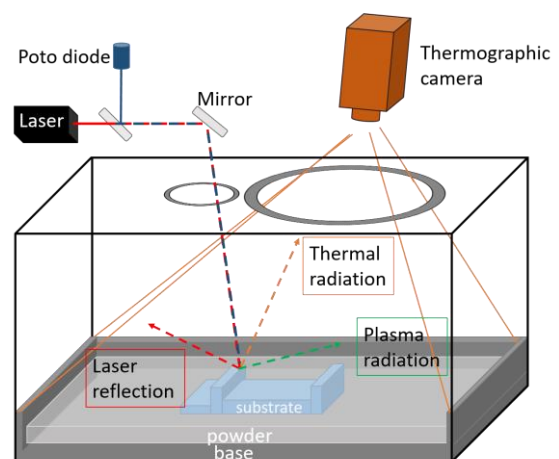


Fig. 1: Principle of process monitoring in selective laser melting (SLM) using optothermal imaging. Capturing thermal radiation data with a thermography camera allows spatial resolution of the thermal properties of the manufactured component.

By integrating LFA into the manufacturing process using Industry 4.0 principles such as real-time data acquisition, manufacturers can improve the quality and performance of their additively manufactured components. Optimal process parameters for SLM can be determined through precise characterization of thermal properties to minimize or correct distortions, cracks, or undesired microstructures.

Method

Laser Flash Analysis is an experimental method for measuring the thermal diffusivity of materials. It was developed in 1961 by Parker et al. [3] and finds wide application in materials science and engineering. The method is based on the principle of transient heat conduction (see Eq. (1) in Tab. 1) and utilizes an intense laser pulse to generate a short-term heating of a thin sample (see Fig. 2). By measuring the temperature change over time at the back side of the sample, the thermal diffusivity of the material can be determined.

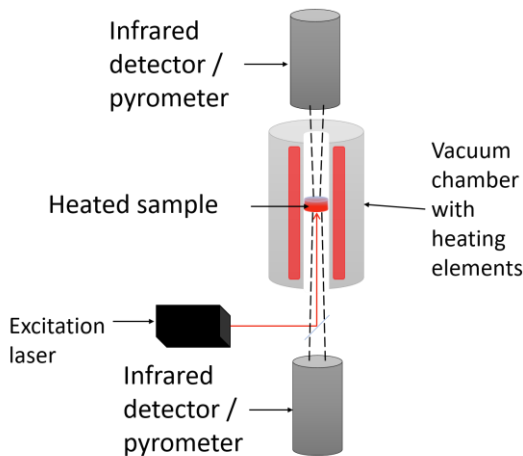


Fig. 2: Principle of laser flash analysis. A heated sample undergoes an additional heat pulse through laser irradiation. In the case of bilateral LFA, an additional detection device is directed towards the front side of the sample.

Tab. 1: First Collection of Equations

(1)	$\frac{dT}{dt} = \alpha \cdot \nabla^2 T(\vec{r}, t)$
(2)	$\Delta T_b = \Delta T(z = d, t) = \Delta T_\infty \cdot \left[1 + 2 \cdot \sum_{n=1}^{\infty} (-1)^n \cdot \exp\left(-\frac{n^2 \cdot \pi^2 \cdot \alpha \cdot t}{d^2}\right) \right]$

(3)	$\Delta T_f = \Delta T(z = 0, t) = \Delta T_\infty \cdot \left[1 + 2 \cdot \sum_{n=1}^{\infty} \exp\left(-\frac{n^2 \cdot \pi^2 \cdot \alpha \cdot t}{d^2}\right) \right]$
-----	---

The fundamental model by Parker et al. solves the transient heat conduction equation under adiabatic assumptions according to [4], which means that heat dissipation from the sample surface is assumed to be negligible. This leads to the solution in Eq. (2) for the temperature increase on the back side of the sample ΔT_b and Eq. (3) for the temperature increase on the front side of the sample ΔT_f , both displayed in Fig. 3.

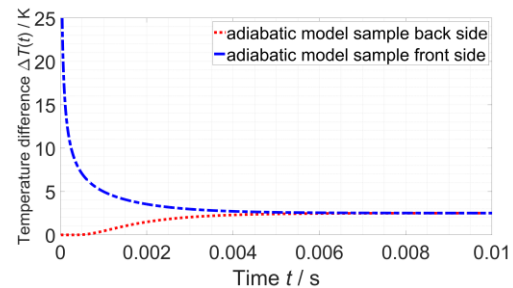


Fig. 3: Exemplary temperature development on the front and back sides of an LFA sample in the adiabatic model.

The temperature rise ΔT_∞ results from the laser energy as well as the sample dimensions and material properties such as density ρ and specific heat capacity c_p . As visible in Fig. 3, the temperature development on the front side of the sample is subject to high dynamics. It is therefore necessary to consider the effects of the laser pulse. While in Parker et al.'s temperature development solution, the temperature rise is the result of a pulse in the form of a delta distribution at time $t = 0$, finite pulse shapes of rectangular pulses (Tab. 2, Eq. (4)) are subsequently considered. Mathematically, this is described by a convolution (Eq. (5)), which leads to the continuous solutions in Eq. (6) and Eq. (7) for the front and back sides of the sample, respectively. An alternative approach is the discrete method. For this, the functions described in Eq. (3) and Eq. (4) are displayed using a time vector with a discrete number of elements, and this output is transformed into the Fourier domain using FFT (Eq. (8)). After multiplication, the inverse transformation into the real space is performed using Eq. (9).

Tab. 2: Second Collection of Equations

(4)	$P_{\Pi}(t) = \begin{cases} P_{\Pi} & \text{for } t_s \leq t \leq t_s + t_p \\ 0 & \text{for } (t_p + t_s) < t, t < t_s \end{cases}$ $Q = \int_{t_s}^{t_s+t_p} P(t) dt = P_{\Pi} \cdot t_p := 1J \rightarrow P_{\Pi} = \frac{1J}{t_p \cdot s}$
(5)	$\Delta T_p = \int_0^{t_s+t_p} P(t') \cdot \Delta T(t-t') dt' =$ $\int_{t_s}^{t_s+t_p} P(t') \cdot \Delta T(t-t') dt'$
(6)	$\Delta T_{f,P_{\Pi}} = \Delta T_{\infty} \cdot$ $\left[1 + \frac{2}{t_p} \cdot \sum_{n=1}^{\infty} \frac{l^2}{\alpha n^2 \pi^2} \cdot \exp\left(-\frac{\alpha n^2 \pi^2 t}{d^2}\right) \cdot \left[\exp\left(\frac{\alpha n^2 \pi^2 t_s}{d^2}\right) \cdot \left(\exp\left(\frac{\alpha n^2 \pi^2 t_p}{d^2}\right) - 1\right) \right] \right]$
(7)	$\Delta T_{b,P_{\Pi}} = \Delta T_{\infty} \cdot$ $\left[1 + \frac{2}{t_p} \cdot \sum_{n=1}^{\infty} (-1)^n \frac{l^2}{\alpha n^2 \pi^2} \cdot \exp\left(-\frac{\alpha n^2 \pi^2 t}{d^2}\right) \cdot \left[\exp\left(\frac{\alpha n^2 \pi^2 t_s}{d^2}\right) \cdot \left(\exp\left(\frac{\alpha n^2 \pi^2 t_p}{d^2}\right) - 1\right) \right] \right]$
(8)	$P_{\Pi,FFT}(k) = FFT(P_{\Pi}(t))$ $\Delta T_{FFT}(k) = FFT(\Delta T(t))$
(9)	$X(k) = P_{\Pi,FFT}(k) \cdot \Delta T_{FFT}(k)$ $\Delta T_{P_{\Pi}}(t) = FFT(X(k))$

Model Examination

By jointly plotting Eq. (6) along with its equivalent in Eq. (9) in Fig. 4, it is evident that both curves converge to ΔT_{∞} as $t \rightarrow \infty$, which serves as an initial plausibility test for both convolution methods. In Fig. 5, focusing on the initial phase of the temperature development allows for a separate examination of the effect of the laser pulse and the agreement of the front side curves. Both convolution methods exhibit consistent behavior here. The temperature on the front side continuously increases from $t = t_s$ until reaching $t = t_s + t_p$. The discontinuous temperature trend for $t > t_s + t_p$ is the result of the abrupt end of the rectangular pulse. However, for the time period $0 < t < t_s$, the plots of the equations do not show physically understandable behavior, as the sample temperature difference does not reach the value of $T=0$. Considering the solution design of Eq. 6 for the real space

convolution and the basic component of the Fourier space solution in Eq. 3, the temperature development curves can by definition not reach the value of $\Delta T = 0$ as the minimum value the curves can converge to is ΔT_{∞} . Therefore, the convolution curves reach a definition limit for $0 < t < t_s$.

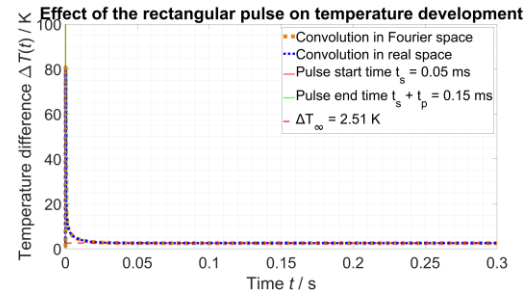


Fig. 4: Display of the convolution models in Fourier and real space for the front side temperature development on the full time scale. Both curves converge to the same value of ΔT_{∞} , which is the same for the non-convolution curves.

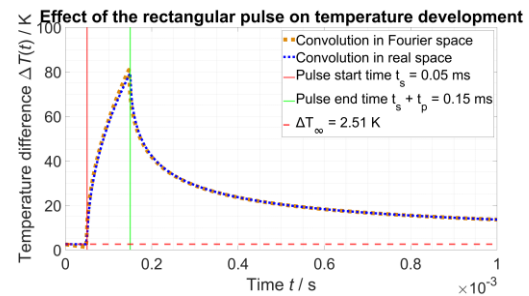


Fig. 5: Display of the convolution models in Fourier and real space for the front side temperature development on the time range near $t = 0$. Both curves show a continuous rise of temperature within the time range of the finite pulse.

Summary and Outlook

Two models have been developed to describe and examine the thermal response of an LFA sample on the side facing the pulse. Through this development, the applicability of LFA for multilayer samples and SLM processes can be extended. In the future, additional pulse shapes will be considered to further optimize the mapping of experimental reality. By fitting curves to captured measurement data, the model will be tested for applicability in the future.

References

- [1] G. Bocchini, G. Bovesecchi, P. Coppa, S. Corasaniti, R. Montanari, and A. Varone, "Thermal diffusivity of sintered steels with flash method at ambient temperature," *International Journal of Thermophysics*, vol. 37, pp. 1-14, 2016; doi: 10.3390/ma12050696
- [2] D. Höflin, C. Sauer, A. Schiffler, and J. Hartmann, "Process Monitoring Using Synchronized Path Infrared Thermography in PBF-LB/M," *Sensors*, vol. 22, no. 16, p. 5943, 2022; doi: 10.3390/s22165943
- [3] W. Parker, R. Jenkins, C. Butler, and G. Abbott, "Flash method of determining thermal diffusivity, heat capacity, and thermal conductivity," *Journal of applied physics*, vol. 32, no. 9, pp. 1679-1684, 1961; doi: 10.1063/1.1728417
- [4] H. S. C. J. C. Jaeger, *Conduction of Heat in Solids*. Oxford: Oxford University Press, 1959, pp. 92-102